[Research Note]

Effect of Oxygen Concentration in NH3-SCR Reaction over Fe- and Cu-loaded Beta Zeolites

Yasuyuki Takamitsu[†1]*, Yuuki Ito[†1], Hiroshi Ogawa[†1], and Tsuneji Sano[†2]

[†1] Nanyo Research Laboratory, Tosoh Corp., Shunan, Yamaguchi 746-8501, JAPAN
[†2] Dept. of Applied Chemistry, Graduate School of Engineering, Hiroshima University, Higashi-Hiroshima 739-8527, JAPAN

The kinetic study on the effect of O_2 concentration in the selective catalytic reduction (SCR) of nitrogen oxide (NO_x) by ammonia (NH_3) was systematically carried out at temperatures below 200 ℃ over Fe- and Cu-loaded beta zeolites. The large difference was observed in the effect of O_2 concentration over the two catalysts: for the Fe-loaded beta zeolite, the NO conversion increased considerably with the O_2 concentration. On the other hand, for the Cu-loaded beta zeolite, increasing the concentration of O_2 did not have a significant impact. In addition, the temperature dependence of the apparent reaction orders was investigated. The apparent reaction order of O_2 decreased with an increase in the reaction temperature, being 0.9 at 150 ℃ and 0.4 at 200 ℃ for the Fe-loaded beta zeolite, and 0.2 at 125 ℃ and 0.1 at 175 ℃ for the Cu-loaded beta zeolite. The fact that the degree of the reduction in the reaction order of O_2 was consisted with that of the increase in the reaction order of NH_3 when the reaction temperature was increased strongly suggests that adsorbed NH_3 inhibits the adsorption of O_2.

1. Introduction

The NH3-SCR of NO is a widely-used method for the removal of NO_x from stationary sources and a variety of suitable transition metal ion-exchanged zeolite catalysts has been developed. The NH3-SCR has also been investigated in recent years as an important candidate for treatment of exhaust fumes from diesel engines. Of the reported transition metal ion-exchanged zeolite catalysts, Fe- and Cu-loaded beta zeolite catalysts have received significant attention due to their high catalytic activity, with differences in the catalytic behaviour of the two catalysts being discussed. Rahkamaa-Tolonen *et al.* have investigated the NH3-SCR of NO over a number of transition metal ion-exchanged beta zeolite catalysts and found that the catalytic activity at temperatures lower than 400 ℃ decreased as follows: Fe＞Cu＞Ag＞H. The loaded metal species served as the active component for catalysing the oxidation of NO to NO_2[1]. Colombo *et al.* have reported notable differences in the NH_3 effect on the NH3-SCR activity between Fe- and Cu-loaded beta zeolite catalysts, namely a negligible effect of NH_3 on the Cu-loaded zeolite and a severe inhibitory effect of NH_3 on the

Fe-loaded zeolite[2]. Fedeyko *et al.* have reported an investigation into the adsorption behaviour of NO_x and NH_3 over Fe- and Cu-loaded beta zeolites by means of an FT-IR technique. In the case of the Fe zeolite catalyst, NH_3 molecules adsorbed on the Fe active sites that would catalyse the oxidation of NO to NO_x species, and severely inhibited the overall NH3-SCR activity. In the presence of NH_3, the IR bands assigned to surface nitrate/nitrite groups, which exhibit the high reactivity with NH_3, were not observed. By contrast, an existence of the nitrate/nitrite groups was apparent for the Cu zeolite catalyst[3].

It has also been reported in the literature that the oxidation of NO to NO_2 is the rate-determining step for the NH3-SCR over Fe-loaded zeolite catalysts[4~8] and that the apparent reaction orders of NO and O_2 are 1 and 0-0.5, respectively[4~6]. The presence of NH_3 suppressed the oxidation of NO to NO_2, leading to reduction in the NH3-SCR activity, with the apparent reaction order of NH_3 being zero or of negative order. The inhibition effect of NH_3 strongly indicates the possibility of NH_3 adsorption onto the active sites[5,9], the reduction of a loaded metal[10], or NH_3 oxidation[6]. On the other hand, for Cu-loaded zeolite catalysts, several rate-determining steps were proposed, such as NO oxidation to NO_2[1,11], oxidative adsorption of NO[12], or oxidation of Cu^+ to Cu^{2+}[13]. The inhibitory effect of NH_3 was

* To whom correspondence should be addressed.
* E-mail: yasuyuki-takamitsu-qs@tosoh.co.jp

not so severe[2),3),12),14),15)]. The apparent reaction orders of NO, O_2, and NH_3 were reported to be 1, 0.5, and zero, respectively[2),12)]. However, as NH_3-SCR kinetic studies have been carried out under considerably different reaction conditions, it is difficult to compare directly and to discuss the differences in the catalytic mechanism for the two zeolite catalysts. In particular, there have been few comparative reports on the difference in the effect of O_2 concentration between the two catalysts.

In this study, in order to obtain further information concerning the difference in the effect of O_2 concentration between the Fe-loaded zeolite and the Cu-loaded zeolite, a systematic kinetic study on the reaction order was carried out.

2. Experimental

2. 1. Preparation and Characterisation of Fe- and Cu-loaded Beta Zeolite Catalysts

The loading of Fe and Cu components onto beta zeolite was carried out by the incipient wetness and the ion-exchange methods, respectively. In general, the ion-exchange method is suitable for loading metal components with a good dispersion. For loading the Fe component, however, difficulties in the preparation of Fe-loaded zeolite with high ion-exchange degrees have been reported[16)]. To investigate the influence of a wide range of metal content, therefore, the incipient wetness method was selected for the Fe-loaded zeolite.

All zeolite catalysts were prepared from the H-form of beta zeolite (Tosoh Corp., Si/Al=14, BET=600 m^2/g). The Fe-loaded beta zeolite catalyst was prepared by the incipient wetness method as follows: an aqueous solution (3.4 mL) of $Fe(NO_3)_3$ (Kishida Chemical Co., Ltd., Japan) was added to the H-form zeolite (10 g) and mixed thoroughly in a ceramic mortar. The resultant wet powder was dried at 110 ℃, followed by calcination at 500 ℃ for 1 h. By contrast, the Cu-loaded beta zeolite catalyst was prepared using the ion-exchange method. The same parent H-form zeolite (10 g) was added to an aqueous solution (100 mL) of $Cu(CH_3COO)_2$ (Kishida Chemical Co., Ltd., Japan) and ammonia and stirred for 2 h at 60 ℃. After filtration, the obtained solid product was dried at 110 ℃ and calcined at 500 ℃ for 1 h.

The contents of Fe and Cu and the Si/Al molar ratio in the prepared zeolite catalysts were determined using an inductively coupled plasma analysis (PerkinElmer Inc., USA, OPTIMA3300DV). Specific surface areas (BET) were measured by N_2 adsorption. The N_2 adsorption isotherm at −196 ℃ was performed using a conventional volumetric apparatus (Beckman Coulter Inc., USA, OMNISORP 360CX). Prior to adsorption measurements, the samples (approximately 0.1 g) were dried at 350 ℃ under vacuum for 2 h. The surface areas were calculated on the basis of 1 g of zeolite by assuming the Fe and Cu species in the calcined catalyst were present as Fe_2O_3 and CuO, respectively. The surface areas of loaded metals were assumed to be negligibly small.

2. 2. NH_3 Temperature-programmed Desorption (TPD) Analysis

One hundred milligrams of sample (powder) was pre-treated under He flow at 500 ℃ for 1 h and then cooled to room temperature. NH_3 adsorption was then performed by flowing a NH_3(10 %)/He mixture through the sample bed at room temperature for 1 h. Afterwards, the system was purged with He at room temperature for 1 h and at 100 ℃ for 1 h. Thereafter, the TPD run was started from 100 ℃ to 500 ℃ at a heating rate of 10 ℃/min in He flow. The gas composition was measured with gas chromatograph (Shimadzu Corp., Japan, GC-9A) equipped with thermal conductivity detector (TCD). The gas flow rate was fixed at 50 mL/min.

2. 3. Temperature-programmed Reduction (TPR) Analysis

Samples (powder) were pre-treated under air flow (50 mL/min) at 500 ℃ for 1 h and then cooled to 100 ℃. The system was purged with H_2(3 %)/N_2 (50 mL/min) at 100 ℃ for 0.5 h. Thereafter, the TPR run was started from 100 ℃ to 700 ℃ at a heating rate of 10 ℃/min in H_2(3 %)/N_2 flow (50 mL/min). The gas composition was monitored with TCD (Shimadzu Corp., Japan, GC-9A).

2. 4. NO TPD Analysis

Samples were pressed and sieved to 600-850 μm in diameter. Two hundred milligrams of sample was pre-treated under N_2 flow (100 mL/min) at 500 ℃ for 1 h and then cooled to room temperature. NO adsorption was then performed by flowing a NO(2.5 %)/N_2 mixture through the sample bed at room temperature at a rate of 100 mL/min for 1 h. Afterwards, the system was purged with N_2 (100 mL/min) at room temperature for 1 h and at 100 ℃ for 0.5 h. Thereafter, the TPD run was started from 100 ℃ to 700 ℃ at a heating rate of 10 ℃/min in N_2 flow (100 mL/min). The gas composition was monitored by FTIR (MIDAC Co., USA, I-4001-F).

2. 5. SCR Activity Tests

The SCR activity measurements were carried out in a fixed-bed flow reactor under atmospheric pressure. Samples were pressed and sieved in order to retain agglomerates of 600-850 μm in diameter. Two hundred milligrams of catalyst was loaded between two layers of inert quartz wool. The reactant gas was composed of 40-310 ppm NO, 0-150 ppm NO_2, 200-800 ppm NH_3, 5-20 % O_2, 1.5-4.5 % H_2O and balance N_2 (NO + NO_2 + NH_3 + O_2 + H_2O + N_2 = 100 %). The gas composition was based on the emissions from diesel engines. The total flow rates were fixed at 800 and

Table 1　Metal Contents and Specific Surface Areas of Fe- and Cu-loaded Beta Zeolites

Catalyst	Metal content [wt%]	BET surface area [m²/g-zeolite]
Fe(0.5)/zeolite	0.5	575
Fe(1.2)/zeolite	1.2	540
Fe(1.9)/zeolite	1.9	536
Fe(3.4)/zeolite	3.4	522
Cu(1.2)/zeolite	1.2	542
Cu(2.3)/zeolite	2.3	562
Cu(3.3)/zeolite	3.3	546
Cu(7.4)/zeolite	7.4	528

Fig. 1　NH₃-TPD Profiles of H-form Zeolite (bold line), Fe(1.9)/Zeolite (solid line), and Cu(3.3)/Zeolite (dashed line)

$1600 \ mL \cdot min^{-1}$ and the GHSV (gas hourly space velocity) values were 90,000 and 180,000 h^{-1}, respectively. During the experiments, the temperature decreased from 500 ℃ to 100 ℃ at 25-50 ℃ intervals. The concentrations of NO, NO_2, N_2O, and NH_3 were analysed by FT-IR spectrometry (MIDAC Co., USA, I-4001-F).

The reaction kinetics were investigated at temperatures around 200 ℃, based on the temperature of exhaust gas emitted from diesel engines (200-500 ℃). At higher reaction temperatures, the diffusion process is the rate-determining step and the catalytic activity is not so significantly different. That is to say, even if there are any differences in the catalytic activity among the prepared catalysts, no difference in the apparent reaction rate is observed. By contrast, at lower temperatures (around 200 ℃) the catalytic reaction is the rate-determining step and the difference in the catalytic activity affects the whole reaction rate.

3. Results and Discussion

3. 1. Catalyst Characterization

The metal contents and the surface areas of Fe- and Cu-loaded beta zeolites are listed in **Table 1**. The samples are labelled as Fe(*n*)/zeolite and Cu(*n*)/zeolite, where *n* is the metal content (wt%). The bulk Si/Al ratio (14) of the beta zeolites did not change after metal loading. For both catalyst samples, the surface area tended to decrease with an increase in the metal content, indicating blocking of zeolitic pores.

Figure 1 shows the NH₃-TPD profiles of H-form zeolite, Fe(1.9)/zeolite, and Cu(3.3)/zeolite. The desorbed amount was compared by removing the effect of the physically adsorbed NH₃, which desorbed at around 200 ℃. The desorption profiles were deconvoluted to two peaks assuming Gaussian peak shapes. The desorbed NH₃ amounts of H-form zeolite, Fe(1.9)/zeolite, and Cu(3.3)/zeolite were 0.66, 0.61, and 0.74 mmol/g-catalyst, respectively. It was suggested that a part of aluminium was removed from the framework during the iron-loading process and that by contrast the dealumination hardly occurs during the copper-loading
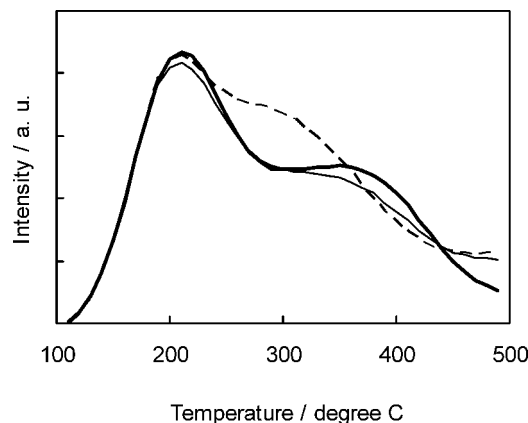
process. The maximum desorption peak around 400 ℃ over Cu/zeolite shifted toward lower temperature as compared with those of the Fe/zeolite and the H-form zeolite, suggesting the weaker NH₃ adsorption on the Cu/zeolite.

Figure 2 shows the H₂-TPR profiles of Fe/zeolites and Cu/zeolites with different metal contents. The Fe/zeolite exhibited one peak at *ca.* 400 ℃, which is associated with the reduction of Fe^{3+} to Fe^{2+}. The reduction temperature was not dependent on the content of iron loaded. The Cu/zeolite exhibited two peaks due to the reduction of Cu^{2+} to Cu^{+} and of Cu^{+} to Cu(metal). Both reduction temperatures decreased with increasing the Cu content, which was consistent with results reported in the literature[17),18)]. For Cu-loaded catalyst, it is considered that the peak at lower temperatures is related to the redox behaviour between Cu^{+} and Cu^{2+}, which would catalyse the NH₃-SCR[19)].

Figure 3 shows the NO-TPD profiles of Fe(1.9)/zeolite and Cu(3.3)/zeolite. Desorption of NO and NO_2 together with a small amount of N_2O (below 1 ppm, not shown) were observed. Two desorption peaks were observed for each component (NO and NO_2). The peak at high temperature is due to the decomposition of nitrate (NO_3^-) or nitrite (NO_2^-)[20),21)]. The peak at low temperature is attributed to the weakly adsorbed NO and NO_2. NO_x ($x \neq 1$) species would be formed during the adsorption process of NO[22)]. Probably, disproportionate of adsorbed NO into N_2O and NO_2 proceeds[23)]. From the fact that N_2O species was hardly detected during the desorption and the purge processes, it might be concluded that generated N_2O decomposed or desorbed before the processes. These results strongly indicate that a portion of NO molecules is adsorbed in an oxidized state. The desorbed amount of NO_x (NO + NO_2) was 0.23 mmol/g-catalyst for Cu(3.3)/zeolite, $NO_x/Cu = 0.44$ mol/mol, and 0.12 mmol/g-catalyst for Fe(1.9)/zeolite, $NO_x/Fe = 0.35$ mol/mol. Taking into account the fact that the
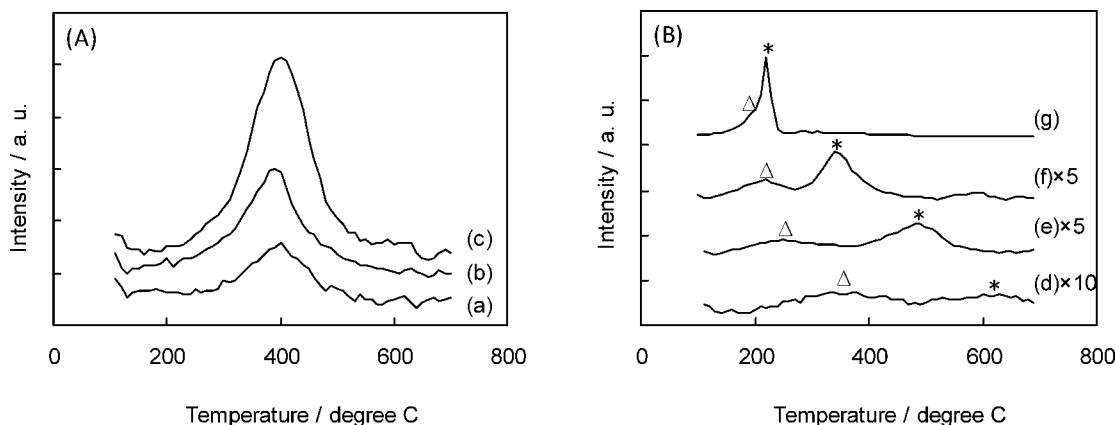
Fe(1.2)/zeolite (a), Fe(1.9)/zeolite (b), Fe(3.4)/zeolite (c), Cu(1.2)/zeolite (d), Cu(2.3)/zeolite (e), Cu(3.3)/zeolite (f), and Cu(7.4)/zeolite (g). The reduction peaks corresponded to Cu^{2+} to Cu^+ and to Cu^+ to Cu(metal) were marked with (△) and (✻), respectively.

Fig. 2　H_2-TPR Profiles of Fe/Zeolite (A) and Cu/Zeolite (B)
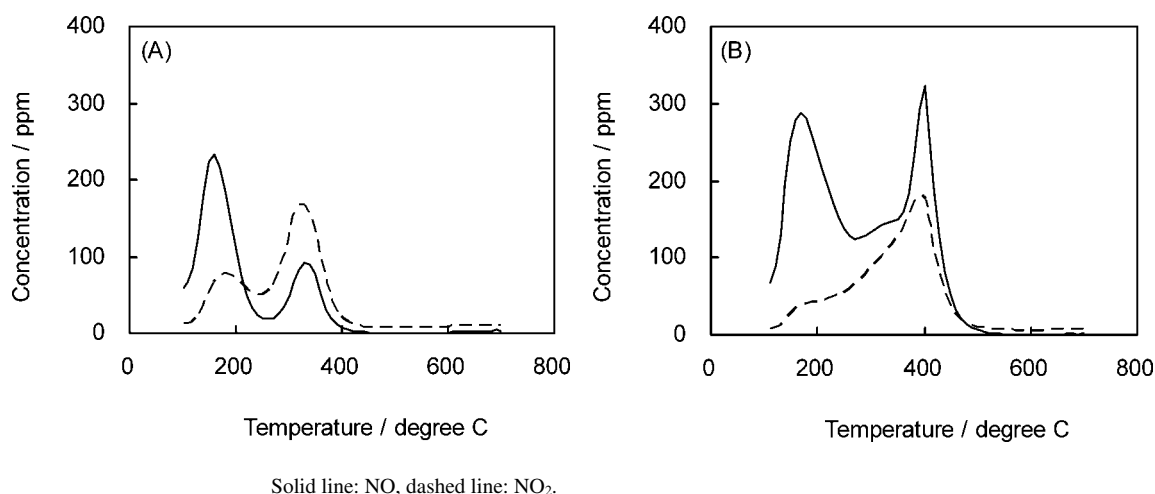
Solid line: NO, dashed line: NO_2.

Fig. 3　NO-TPD Profiles of Fe(1.9)/Zeolite (A) and Cu(3.3)/Zeolite (B)

desorption temperatures of NO and NO_2 from Cu(3.3)/zeolite were higher than those from Fe(1.9)/zeolite, it can be concluded that NO molecules adsorb more strongly on Cu(3.3)/zeolite as compared to Fe(1.9)/zeolite.

3. 2.　NH₃-SCR

Figure 4 shows the NH₃-SCR activities of Fe/zeolite and Cu/zeolite catalysts with various metal contents. The Cu/zeolite catalysts exhibited the higher NO conversions at low temperatures as compared to the Fe/zeolite catalysts. However, the NO conversions on the Cu/zeolite catalysts at 500 ℃ were lower. Additionally, it was found that the NO conversion on the Cu/zeolite catalysts increased with the Cu content and became constant at 3 wt% of Cu.

On the other hand, for the Fe/zeolite catalysts, the NO conversion increased with the Fe content and reached a maximum value at 1-2 wt% of Fe. Although clear dif-

ference in the peak position of the maximum reduction temperature on H₂-TPR profile was hardly observed among Fe-loaded zeolites with the Fe content 1-3 wt%, this indicates that the NH₃-SCR activity is dependent on the amount of isolated Fe species. Excess Fe loading yields metal aggregates, thereby reducing the SCR activity[24]~[26]. As a result, optimisation of metal content is required for the preparation of a high performance metal-loaded zeolite catalyst. Therefore, Fe(1.9)/zeolite and Cu(3.3)/zeolite were selected in the following catalytic tests.

Figure 5 shows the concentrations of NO, NH₃, and N₂O over Fe(1.9)/zeolite and Cu(3.3)/zeolite catalysts. The concentrations of NO and NH₃ at low temperatures below 300 ℃ decreased in the similar trend. However, at high temperatures more than 400 ℃, the considerable amount of unreacted NO was detected for the Cu/zeolite in regardless of the detection of a trace amount
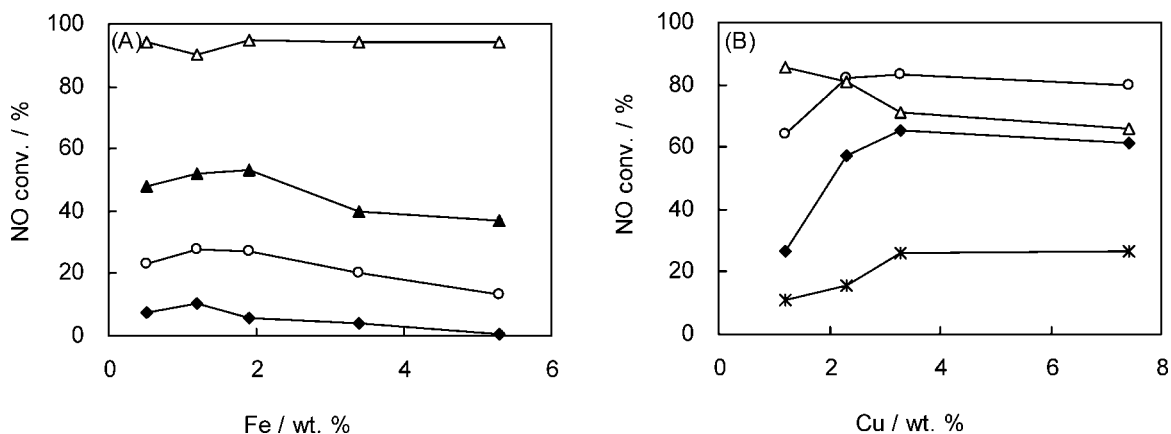
Reaction conditions: 200 ppm NO, 200 ppm NH₃, 10 % O₂, 3 % H₂O, balance N₂.   Temp.: 500 ℃ (△), 200 ℃ (▲), 175 ℃ (○),
150 ℃ (◆), 125 ℃ (✳).   GHSV: 90,000 h⁻¹.

Fig. 4   NO Conversion as a Function of Metal Content over Fe/Zeolite (A) and Cu/Zeolite (B)
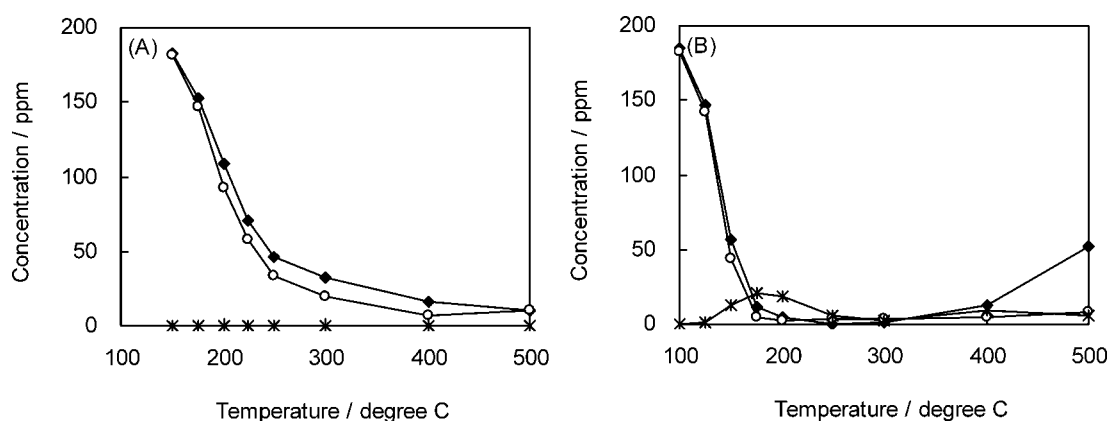
Reaction conditions: 200 ppm NO, 200 ppm NH₃, 10 % O₂, 3 % H₂O, balance N₂.   GHSV: 90,000 h⁻¹.

Fig. 5   NO (◆), NH₃ (○), and N₂O (✳) Concentrations as a Function of Temperature over Fe(1.9)/Zeolite (A) and Cu(3.3)/
Zeolite (B)

of NH₃.   NH₃ would be oxidized by O₂ and the NH₃-SCR would not take place effectively[15].   The detection of N₂O on the Cu/zeolite indicates the presence of side reaction[27].   In the following kinetic study, the reaction rate of the NH₃-SCR was calculated using the Eq. (1):

$$r = r_{NO} - r_{N_2O} \qquad (1)$$

where r is the total NH₃-SCR rate (mol·s⁻¹·kg-cat⁻¹), r_{NO} is the NO conversion rate (mol-NO s⁻¹·kg-cat⁻¹), and r_{N_2O} is the N₂O formation rate (mol-N₂O s⁻¹·kg-cat⁻¹).   Since N₂O is also consumed in the SCR, the exact evaluation of r_{N_2O} is difficult.   Here the detected N₂O is assumed to be regarded as the whole N₂O formed in the reaction.

In order to obtain further insight into the differences in reaction behaviour between the Fe/zeolite and the Cu/zeolite, the kinetic study focused especially on the reaction order.   The concentrations of O₂, NO, NH₃, and H₂O were varied systematically.   **Figures 6-9** show the concentration dependence of NH₃-SCR activity.   The positive O₂ concentration dependence was observed for both catalysts (**Fig. 6**); namely, a remarkable increase in the reaction rate at the high O₂ concentration for the Fe/zeolite catalyst, and only the slight enhancement for the Cu/zeolite catalyst.   The reaction rate increased proportionally with the NO concentration (**Fig. 7**) for both Fe/zeolite and Cu/zeolite catalysts.   As can be seen in **Fig. 8**, however, the reaction rate decreased with the NH₃ concentration although the degree of reduction differed between the two catalysts.   The inhibition effect of NH₃ over the Fe/zeolite was stronger than that over the Cu/zeolite[2].   H₂O also showed the negative concentration dependence.   The reaction rate decreased slightly at the high H₂O concentration (**Fig. 9**).

On the basis of these results, the apparent reaction

62
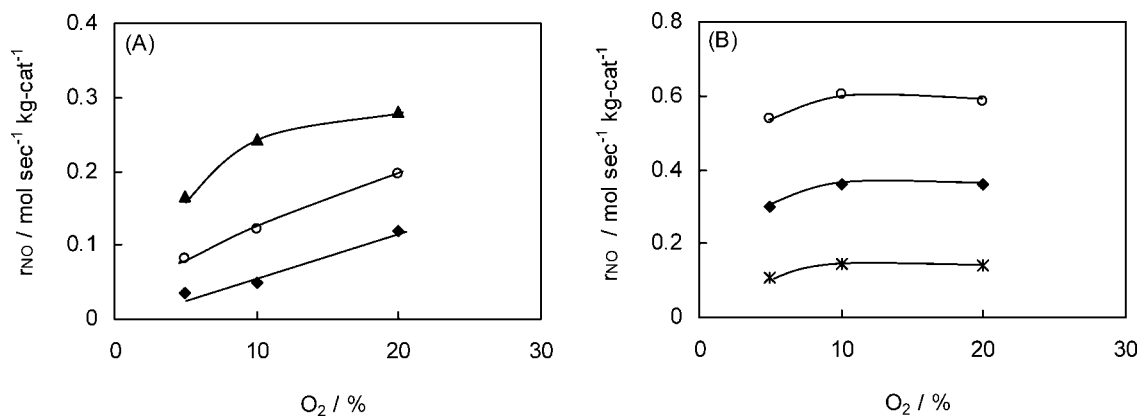
Reaction conditions: 200 ppm NO, 200 ppm NH₃, 3 % H₂O, balance N₂. Temp.: 200 ℃ (▲), 175 ℃ (○), 150 ℃ (◆), 125 ℃ (＊).
GHSV: 90,000 h⁻¹ (A), 180,000 h⁻¹ (B).

Fig. 6   NO Reaction Rate as a Function of O₂ Concentration over Fe(1.9)/Zeolite (A) and Cu(3.3)/Zeolite (B)
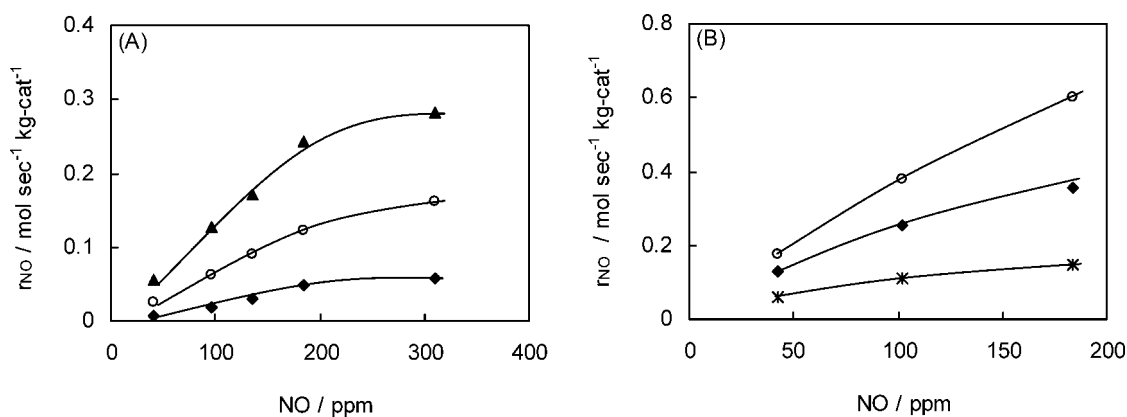
Reaction conditions: 200 ppm NH₃, 10 % O₂, 3 % H₂O, balance N₂. Temp.: 200 ℃ (▲), 175 ℃ (○), 150 ℃ (◆), 125 ℃ (＊).
GHSV: 90,000 h⁻¹ (A), 180,000 h⁻¹ (B).

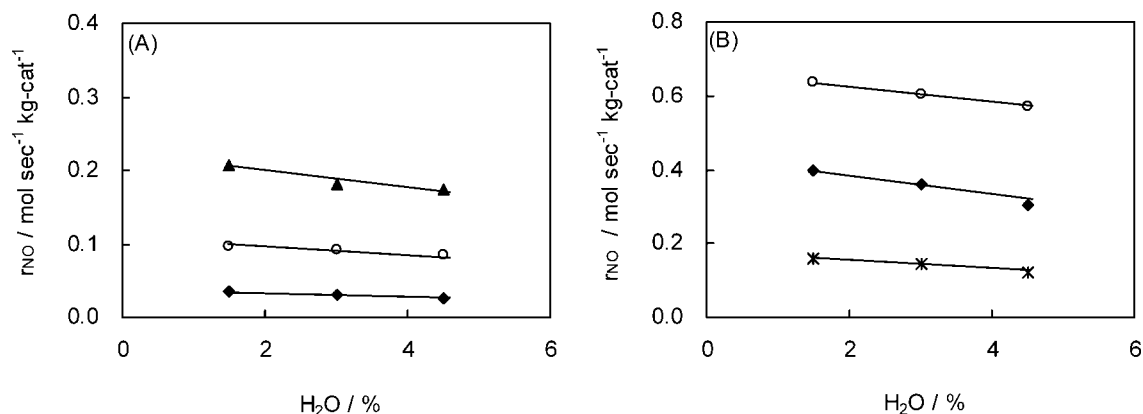Fig. 7   NO Reaction Rate as a Function of NO Concentration over Fe(1.9)/Zeolite (A) and Cu(3.3)/Zeolite (B)
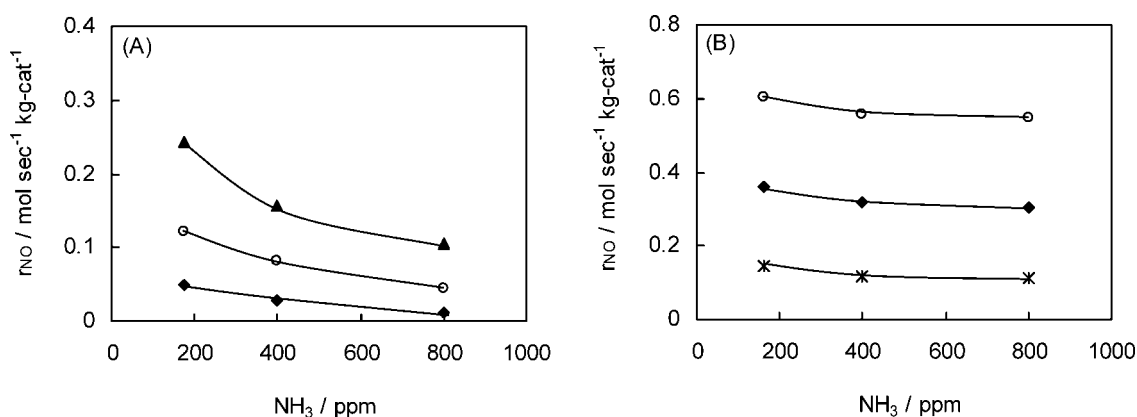
Reaction conditions: 200 ppm NO, 10 % O₂, 3 % H₂O, balance N₂. Temp.: 200 ℃ (▲), 175 ℃ (○), 150 ℃ (◆), 125 ℃ (＊).
GHSV: 90,000 h⁻¹ (A), 180,000 h⁻¹ (B).

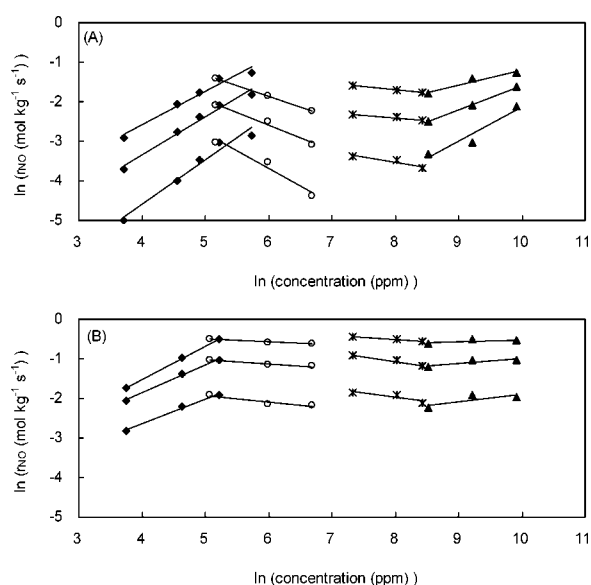Fig. 8   NO Reaction Rate as a Function of NH₃ Concentration over Fe(1.9)/Zeolite (A) and Cu(3.3)/Zeolite (B)

Reaction conditions: 200 ppm NO, 200 ppm NH₃, 10 % O₂, balance N₂. Temp.: 200 ℃ (▲), 175 ℃ (○), 150 ℃ (◆), 125 ℃ (*).
GHSV: 90,000 h⁻¹ (A), 180,000 h⁻¹ (B).

Fig. 9 NO Reaction Rate as a Function of H₂O Concentration over Fe(1.9)/Zeolite (A) and Cu(3.3)/Zeolite (B)

The straight lines were fitted by the least square method.
(A) Fe(1.9)/zeolite: $T = 200$ (upper line), 175 (middle line), 150 (lower line) ℃, GHSV: 90,000 h⁻¹.
(B) Cu(3.3)/zeolite: $T = 175$, 150, 125 ℃, GHSV: 180,000 h⁻¹.
Reaction conditions: 40-310 ppm NO, 200-800 ppm NH₃, 5-20 % O₂, 1.5-4.5 % H₂O, and balance N₂.

Fig. 10 Log-log Plots of Reaction Rate *vs.* Concentrations of NO (◆), NH₃ (○), O₂ (▲) and H₂O (*)

orders of O₂, NO, NH₃, and H₂O were determined by the log-log plots of the gas concentration and the reaction rate (r), as seen in **Fig. 10**. The apparent reaction orders were defined by the Eq. (2):

$$r = k_1\, C_{NO}{}^a\, C_{NH_3}{}^b\, C_{O_2}{}^c\, C_{H_2O}{}^d \qquad (2)$$

where r is the NH₃-SCR reaction rate (mol·s⁻¹·kg-cat⁻¹), C is the concentration (ppm), k_1 is the apparent rate constant, and a, b, c and d are the apparent reaction

orders of NO, NH₃, O₂, and H₂O, respectively. To avoid the mass transfer resistance, for the most part NO conversions were set to be less than 30 % except for NO conversions over Cu(3.3)/zeolite at 175 ℃. The temperature dependences of the apparent reaction orders of NO, NH₃, O₂, and H₂O are summarised in **Fig. 11**. The large difference in the apparent reaction order of O₂ was observed between the Fe/zeolite and the Cu/zeolite catalysts. For the Fe/zeolite catalyst, the reaction order of O₂ decreased with an increase in the reaction temperature, being 0.9 at 150 ℃ and 0.4 at 200 ℃. The reaction orders of NO and O₂ at 200 ℃ were similar to the values reported in the literature (1 (NO) and 0.5 (O₂)), suggesting that the rate-determining step in the present reaction conditions is the oxidation of NO. However, the reaction order of O₂ at 150 ℃ significantly exceeded 0.5, suggesting a possibility of the different rate-determining step (described later). The apparent reaction order of NO in the Cu/zeolite case increased with the reaction temperature, from 0.6 (125 ℃) to 0.9 (175 ℃). On the other hand, the apparent reaction order of NO on Fe/zeolite decreased from 1.1 (150 ℃) to 0.8 (200 ℃). The low reaction order of NO for the Cu/zeolite catalyst is probably indicative of stronger NO adsorption, which is consistent with the result of the NO-TPD, as shown in **Fig. 3**. The apparent reaction order of NH₃ increased with the reaction temperature, although the degree of the increase was different between the two catalysts. The weaker inhibition effect of NH₃ at higher temperatures suggests adsorption of NH₃ on the active sites, which catalyse the NH₃-SCR. The apparent reaction order of H₂O slightly increased with the reaction temperature, from −0.3 (150 ℃) to −0.1 (200 ℃) for the Fe/zeolite and from −0.2 (150 ℃) to −0.1 (200 ℃) for the Cu/zeolite. However, the value of the apparent reaction order of H₂O was hardly dependent on the kind of loaded metal.
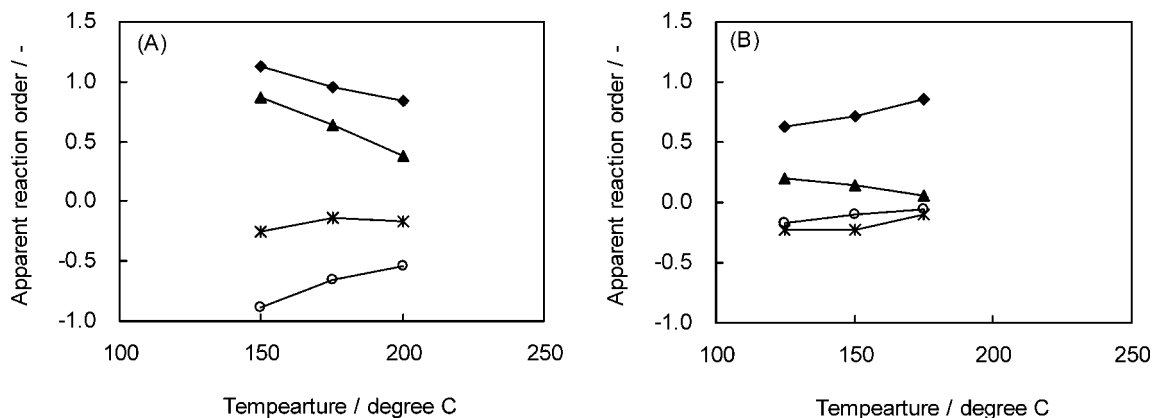
$r_{NO} = k_1 C_{NO}{}^a C_{NH_3}{}^b C_{O_2}{}^c C_{H_2O}{}^d$.　a (◆), b (○), c (▲), d (✳).

Fig. 11　Apparent Reaction Orders of NO, O₂, NH₃ and H₂O as a Function of Temperature over Fe(1.9)/Zeolite (A) and Cu(3.3)/Zeolite (B)
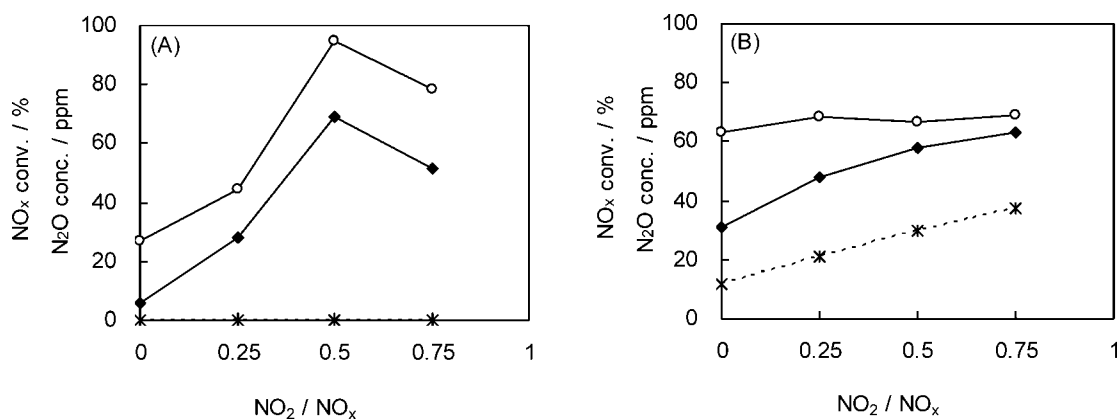
Reaction conditions: 200 ppm NO$_x$ (NO + NO₂), 200 ppm NH₃, 10 % O₂, 3 % H₂O, balance N₂.　Temp.: 175 ℃ (○, ✳), 150 ℃ (◆).　GHSV: 90,000 h⁻¹ (A), 180,000 h⁻¹ (B).

Fig. 12　NO$_x$ Conversion (○, ◆) and N₂O Concentration (✳) as a Function of NO₂/NO$_x$ Ratio over Fe(1.9)/Zeolite (A) and Cu(3.3)/Zeolite (B)

Many reports have dealt with the enhancement of the NH₃-SCR rate over metal loaded zeolite catalysts by addition of NO₂ into the feed[1),4),8),15),28)]. The remarkable enhancement of the reaction rate is observed at the condition of NO₂/NO$_x$ = 0.5 (so called "fast SCR," NO + NO₂ + 2NH₃ → 2N₂ + 3H₂O). **Figure 12** shows the relationship between NO$_x$ conversion and the NO₂/NO$_x$ (NO$_x$ = NO + NO₂) ratio in the feed. The NO$_x$ conversion was calculated using the Eq. (3)

$$NO_x \text{ conv.} = \left(1 - \frac{\text{outletNO} + \text{outletNO}_2 + \text{outletN}_2\text{O}}{\text{inletNO} + \text{inletNO}_2}\right) \times 100$$

(3)

The marked enhancement of the NO$_x$ conversion on the Fe/zeolite was observed as compared to the Cu/zeolite[2),3)]. Taking into account the fact that the oxidation ability of the Cu/zeolite is higher than that of the Fe/zeolite (the reduction temperature of Cu²⁺ to Cu⁺

(230 ℃) was lower than that of Fe³⁺ to Fe²⁺ (390 ℃), as shown in **Fig. 2**(f) and (b).), it is reasonable to assume that NO₂ is easily produced on the Cu/zeolite catalyst by oxidation of NO, resulting in only a small influence of additionally introduced NO₂. Furthermore, increased N₂O production occurred with increasing the NO₂/NO$_x$ ratio on the Cu/zeolite. This side reaction also weakened the effect of NO₂ addition.

3. 3.　Inhibition Effect of NH₃ on O₂ Adsorption

As described above, there were some differences in the reaction behaviour between the Fe/zeolite and the Cu/zeolite, notably, the reaction orders of O₂ and NH₃. The reaction order of O₂ for the Fe/zeolite was higher than that for the Cu/zeolite. Low reaction orders of O₂ are often observed for catalysts on which the loaded metal is easily oxidized or onto which O₂ can easily adsorb. Taking into account the results of O₂-TPD reported in the literature[29),30)] and the standard enthalpy

change of formation of metal oxides, Fe species adsorb O_2 more strongly and tend to be oxidized more easily than Cu species, suggesting a lower reaction order of O_2 for the Fe/zeolite catalyst. However, the opposite phenomenon was observed in the present work. Therefore, the difference in the reaction order of O_2 would be attributed not only to the interaction between O_2 and the catalyst but also to the presence of other gas components. Focusing on the temperature dependence of the reaction orders (**Fig. 11**), the absolute value of the slope for O_2 is almost the same as that for NH_3 for both catalysts, implying that the reaction order of O_2 is affected by the competitive adsorption of NH_3 and O_2. In other words, NH_3 adsorbs strongly and exclusively on the Fe/zeolite, thus inhibiting O_2 adsorption, while NH_3 does not strongly inhibit O_2 adsorption on the Cu/zeolite. This is supported by the lower desorption temperature in the NH_3-TPD curve of Cu/zeolite. Owing to limited data, we could not clearly explain the whole results at the present time. However, it is worth noting the possibility of competitive adsorption of NH_3 and O_2. Although the inhibition effect of NH_3 on NH_3-SCR has been widely reported[5),9),15),31)], it has usually been attributed to the competitive adsorption of NH_3 and NO_x.

The high reaction order of O_2 (above 0.5) for the Fe/zeolite could be explained as follows. The SCR reaction over H-form zeolite is first order with respect to O_2 concentration[31),32)]. Since the dissociative adsorption of O_2 does not occur on H-form zeolite without a loaded metal, it is considered that molecular oxygen reacts directly with NO. In the case of the Fe/zeolite, as the strongly adsorbed NH_3 might inhibit the dissociative adsorption of O_2, molecular oxygen reacted directly with NO in a similar manner, resulting in the high reaction order of O_2 at low temperatures.

The decrease in the reaction order of O_2 at high temperature (200 ℃) over the Fe/zeolite catalyst can be rationalised by assuming that (a) there is an increase in the amount of molecular O_2 on the catalyst surface that can react with NO, or (b) NO reacts with dissociatively adsorbed O_2. In the present case, the assumption (b) appears plausible as N_2O_3 is thought to be the desirable intermediate on the NH_3-SCR[4),33),34)]. **Figure 12** also indicates that N_2O_3 would be the desirable intermediate over the Fe/zeolite even at 150 ℃ because the NO conversion has the maximum at $NO_2/NO_x = 0.5$. Considering the assumption (b), N_2O_3 could be formed by the reaction of NO with NO_2. However, in the assumption (a), nitrates would be formed instead of N_2O_3, and the formation of nitrates would be an undesirable reaction path.

3. 4. Difference in Catalytic Behaviour between Fe/Zeolite and Cu/Zeolite

The similar reaction orders of NH_3-SCR were observed for both the Fe- and the Cu-loaded zeolites,

namely, about first order for NO, positive for O_2 and negative for NH_3 and H_2O. This suggests that the basic reactions proceed in a similar manner on both catalysts[28)]. As the reaction order of O_2 was positive, the adsorbed O_2 must be involved in the rate-determining step. In the step, the gaseous or the adsorbed NO reacts with the adsorbed O_2 to form adsorbed NO_x species. NH_3 adsorbed on the catalyst surface would prevent adsorption of O_2. This model is consistent with the observed adsorption behaviour of NO_x and NH_3 on metal loaded zeolite[3)]. The main difference between two zeolite catalysts is the difference in the reaction orders of NH_3 and O_2. The reaction orders would reflect the strength of the NH_3 adsorption, which inhibited the O_2 adsorption. The interaction of the gases and catalysts were dependent on the kind of loaded metals.

From the experimental results with addition of NO_2, it was also suggested that the high catalytic activity of the Cu/zeolite at low temperatures would be due to its high NO oxidation ability[1),11)]. However, in the case of a strong oxidizing agent like NO_2, the Cu/zeolite not only loses its advantage but also shows lower catalytic activity due to undesired side reaction (N_2O generation) as compared with the Fe/zeolite.

4. Conclusions

The kinetic study on the reaction order of NH_3-SCR over Fe- and Cu-loaded zeolites was carried out systematically. From the results of the temperature dependence of the apparent reaction orders, it is found that the NH_3-SCR is strongly inhibited by NH_3 and accelerated by O_2 over the Fe/zeolite. By contrast, only the slight inhibition by NH_3 and the slight enhancement by O_2 are observed for the Cu/zeolite. The inhibition effect of NH_3 is due to the competitive adsorption of NH_3 and O_2.

References

1) Rahkamaa-Tolonen, K., Maunula, T., Lomma, M., Huuhtanen, M., Keiski, R. L., *Catal. Today*, **100**, 217 (2005).
2) Colombo, M., Nova, I., Tronconi, E., *Catal. Today*, **151**, 223 (2010).
3) Fedeyko, J. M., Chen, B., Chen, H.-Y., *Catal. Today*, **151**, 231 (2010).
4) Brandenberger, S., Kröcher, O., Tissler, A., Althoff, R., *Catal. Rev.*, **50**, 492 (2008).
5) Iwasaki, M., Yamazaki, K., Shinjoh, H., *Appl. Catal. A: General*, **366**, 84 (2009).
6) Huang, H. Y., Long, R. Q., Yang, R. T., *Appl. Catal. A: General*, **235**, 241 (2002).
7) Delahay, G., Valade, D., Guzmán-Vargas, A., Coq, B., *Appl. Catal. B: Environment*, **55**, 149 (2005).
8) Long, R. Q., Yang, R. T., *J. Catal.*, **207**, 224 (2002).
9) Kröcher, O., Devadas, M., Elsener, M., Wokaun, A., Söger, N., Pfeifer, M., Demel, Y., Mussmann, L., *Appl. Catal. B: Environment*, **66**, 208 (2006).
10) Devadas, M., Kröcher, O., Elsener, M., Wokaun, A., Mitrikas,

G., Söger, N., Pfeifer, M., Demel, Y., Mussmann, L., *Catal. Today*, **119**, 137 (2007).

11) Moden, B., Donohue, J. M., Cormier, W. E., Li, H.-X., Proc. of 4th International FEZA Conference, 1219 (2008).

12) Komatsu, T., Nunokawa, M., Moon, I. S., Takahara, T., Namba, S., Yashima, T., *J. Catal.*, **148**, 427 (1994).

13) Goursot, A., Coq, B., Fajula, F., *J. Catal.*, **216**, 324 (2003).

14) Delahay, G., Kieger, S., Tanchoux, N., Trens, P., Coq, B., *Appl. Catal. B: Environment*, **52**, 251 (2004).

15) Sjövall, H., Olsson, L., Fridell, E., Blint, R. J., *Appl. Catal. B: Environment*, **64**, 180 (2006).

16) Feng, X., Hall, W. K., *J. Catal.*, **166**, 368 (1997).

17) Bulánek, R., Wichterlová, B., Sobalík, Z., Tichý, J., *Appl. Catal. B: Environment*, **31**, 13 (2001).

18) Castagnola, N. B., Kropf, A. J., Marchall, C. L., *Appl. Catal. A: General*, **290**, 110 (2005).

19) Cheung, T., Bhargava, S. K., Hobday, M., Foger, K., *J. Catal.*, **158**, 301 (1996).

20) Torre-Abreu, C., Ribeiro, M. F., Henriques, C., Delahay, G., *Appl. Catal. B: Environment*, **12**, 249 (1997).

21) Zhang, W. X., Yahiro, H., Mizuno, N., Izumi, J., Iwamoto, M., *Langmuir*, **9**, 2337 (1993).

22) Varga, J., Fudala, Á., Halász, J., Schöbel, G., Kiricsi, I., *Stud. Surf. Sci. Catal.*, **94**, 665 (1995).

23) Li, Y., Armor, J. N., *Appl. Catal.*, **76**, L1 (1991).

24) Kogel, M., Monnig, R., Schwieger, W., Tissler, A., Turek, T., *J. Catal.*, **182**, 470 (1999).

25) Høj, M., Beier, M. J., Grunwaldt, J., Dahl, S., *Appl. Catal. B: Environment*, **93**, 166 (2009).

26) Brandenberger, S., Kröcher, O., Tissler, A., Althoff, R., *Appl. Catal. B: Environment*, **95**, 348 (2010).

27) Delahay, G., Coq, B., Kieger, S., Neveu, B., *Catal. Today*, **54**, 431 (1999).

28) Sjövall, H., Blint, R. J., Gopinath, A., Olsson, L., *Ind. Eng. Chem. Res.*, **49**, 39 (2010).

29) Kameoka, S., Nobukawa, T., Takana, S., Ito, S., Tomishige, K., Kunimori, K., *Phys. Chem. Chem. Phys.*, **5**, 3328 (2003).

30) Wang, Z., Sklyarov, A. V., Keulks, G. W., *Catal. Today*, **33**, 291 (1997).

31) Stevenson, S. A., Vartuli, J. C., Brooks, C. F., *J. Catal.*, **190**, 228 (2000).

32) Eng, J., Bartholomew, C. H., *J. Catal.*, **171**, 14 (1997).

33) Long, R. Q., Yang, R. T., *J. Catal.*, **194**, 80 (2000).

34) Chen, H., Sun, Q., Wen, B., Yeom, Y., Weitz, E., Sachtler, W. M. H., *Catal. Today*, **1**, 1 (2004).

···

要　　旨

鉄および銅担持ベータ型ゼオライト触媒上のアンモニア SCR における酸素濃度の影響

高光　泰之[†1]，伊藤　悠軌[†1]，小川　　宏[†1]，佐野　庸治[†2]

[†1] 東ソー(株)南陽研究所，746-8501 山口県周南市開成町4560

[†2] 広島大学大学院工学研究院応用化学専攻，739-8527 広島県東広島市鏡山1-4-1

　鉄および銅担持ベータ型ゼオライトを用いて，アンモニア SCR における酸素濃度の影響を調査した。両者で酸素濃度の影響は大きく異なっており，酸素濃度を5％から20％まで高くすると，鉄担持ゼオライトでは反応速度が顕著に上昇したが，銅担持ゼオライトでは反応速度の変化は小さかった。反応次数の温度依存性を調査したところ，いずれの触媒においても温度上昇に伴い見かけの酸素次数は低下した。鉄担持ゼオライトでは0.9次が0.4次に（150→200℃），銅担持ゼオライトでは0.2次が0.1次に変化した（125→175℃）。温度上昇に伴う酸素次数の低下幅はアンモニア次数の上昇幅と一致しており，律速過程においてアンモニアが酸素の吸着を阻害していることが示唆された。

···